Published OnlineFirst September 21, 2010; DOI:10.1158/0008-5472.CAN-10-2353

Cancer Research

Epidermal Growth Factor Receptor Expression Identifies Functionally and Molecularly Distinct Tumor-Initiating Cells in Human Glioblastoma Multiforme and Is Required for Gliomagenesis

Stefania Mazzoleni, Letterio S. Politi, Mauro Pala, et al.

Cancer Res 2010;70:7500-7513. Published OnlineFirst September 21, 2010.

Published OnlineFirst September 21, 2010; DOI:10.1158/0008-5472.CAN-10-2353

Cancer Research

Epidermal Growth Factor Receptor Expression Identifies Functionally and Molecularly Distinct Tumor-Initiating Cells in Human Glioblastoma Multiforme and Is Required for Gliomagenesis

Stefania Mazzoleni[1,5], Letterio S. Politi[2], Mauro Pala[6], Manuela Cominelli[7], Alberto Franzin[3], Lucia Sergi Sergi[4], Andrea Falini[2], Michele De Palma[4], Alessandro Bulfone[6], Pietro L. Poliani[7], and Rossella Galli[1]

Abstract

Epidermal growth factor receptor (EGFR) is a known diagnostic and, although controversial, prognostic marker of human glioblastoma multiforme (GBM). However, its functional role and biological significance in GBM remain elusive. Here, we show that multiple GBM cell subpopulations could be purified from the specimens of patients with GBM and from cancer stem cell (CSC) lines based on the expression of EGFR and of other putative CSC markers. All these subpopulations are molecularly and functionally distinct, are tumorigenic, and need to express EGFR to promote experimental tumorigenesis. Among them, EGFR-expressing tumor-initiating cells (TIC) display the most malignant functional and molecular phenotype. Accordingly, modulation of EGFR expression by gain-of-function and loss-of-function strategies in GBM CSC lines enhances and reduces their tumorigenic ability, respectively, suggesting that EGFR plays a fundamental role in gliomagenesis. These findings open up the possibility of new therapeutically relevant scenarios, as the presence of functionally heterogeneous $EGFR^{pos}$ and $EGFR^{neg}$ TIC subpopulations within the same tumor might affect clinical response to treatment. *Cancer Res; 70(19); 7500–13. ©2010 AACR.*

Introduction

In the last 10 years, the identification of putative cancer stem cells (CSC) in different types of tumors has raised many expectations. CSCs represent a rare fraction of the tumor bulk, uniquely responsible for tumor initiation and progression and, as such, are envisioned as elective targets of therapy (1, 2). The CSC model of tumorigenesis has been convincingly validated in many hemopoietic malignancies (3) and in solid tumors such as breast and colon cancers (4–7). However, in other tumors, CSCs seem to make up the majority of cells within the tumor bulk and all exhibit tumor-initiating ability, thus being more appropriately called tumor-initiating cells (TIC; refs. 8–11).

This last model might also apply to glioblastoma multiforme (GBM), as soundly shown by recent studies in cultured CSC lines (12, 13). To test whether this concept might hold true in specimens from patients with primary GBM, we selected the epidermal growth factor receptor (EGFR) as a prospective GBM CSC marker (14, 15). EGFR expression in GBM has both diagnostic and prognostic significance (16–19) and it is associated with tumor progression (20). Likewise, *EGFR* gene amplification is positively correlated with molecularly defined GBM subclasses, characterized by active proliferation and poor prognosis (21). Valuable preclinical information has also been obtained by modulating EGFR expression in standard serum-cultured glioma cell lines (22–25) and by using these *in vitro* cultures for testing different therapeutic approaches (26).

Here, we investigated the biological significance of EGFR expression in human primary GBM by assessing its functional role in tumor cell fractions purified from several GBM patient–derived specimens and by validating it in GBM CSC lines, which reproduce the genotypic and phenotypic characteristics of GBM more faithfully than standard glioma cell lines (27, 28). By this experimental strategy, we identified multiple subpopulations of GBM TICs, each characterized by a distinct gene signature and tumorigenic potential, and thus being able to reproduce the diverse pathologic and functional features of GBM, such as invasive and angiogenic behavior.

Authors' Affiliations: [1]Neural Stem Cell Biology Unit, Division of Regenerative Medicine, Stem Cells and Gene Therapy, [2]Neuroradiology Unit and CERMAC, [3]Neurosurgery Unit, and [4]Angiogenesis and Tumor Targeting Research Unit, Telethon Institute for Gene Therapy, Division of Regenerative Medicine, Stem Cells and Gene Therapy, San Raffaele Scientific Institute; [5]Vita-Salute San Raffaele University, Milan, Italy; [6]Bio))flag Ltd., Pula, Cagliari, Italy; and [7]Department of Pathology, University of Brescia-Spedali Civili of Brescia, Brescia, Italy

Note: Supplementary data for this article are available at Cancer Research Online (http://cancerres.aacrjournals.org/).

Corresponding Author: Rossella Galli, Neural Stem Cell Biology Unit, Division of Regenerative Medicine, Stem Cells and Gene Therapy, San Raffaele Scientific Institute, Via Olgettina 58, 20132 Milan, Italy. Phone: 39-02-2643-4626; Fax: 39-02-2643-4621; E-mail: galli.rossella@hsr.it.

doi: 10.1158/0008-5472.CAN-10-2353

Published OnlineFirst September 21, 2010; DOI:10.1158/0008-5472.CAN-10-2353

Our findings unequivocally associate EGFR expression with specific biological functions and molecular traits in distinct GBM cell subpopulations, thus providing relevant preclinical information to be exploited for the development of TIC subpopulation–targeted effective therapies.

Materials and Methods

Collection and processing of patients' specimens

GBM specimens were collected from patients with histologic diagnosis of primary GBM (WHO grade 4 glioma) in accordance with the protocol approved by the institutional review board of San Raffaele Scientific Institute (01-CSC07). Tumor diagnosis and grading were blind-reviewed by different pathologists at two distinct institutions. Samples that did not satisfy the inclusion criteria of primary GBMs (e.g., GBM with oligodendroglioma features) were excluded from the study. See Supplementary Experimental Procedure for processing methods.

Immunohistochemical staining

Four-micrometer sections were cut from paraffin blocks and were stained with mouse antihuman EGFR, mouse anti-CD31 (all DakoCytomation), rabbit anti-SOX2 (Abcam), mouse anti-Bmi1, and mouse anti-CD15 (Becton Dickinson). Sections were then incubated with a secondary antibody (ChemMATE Envision Rabbit/Mouse, DakoCytomation).

Molecular analysis

Total RNA from GBM tumor specimens and from CSC lines was extracted using the RNeasy Micro and Mini Kits (Qiagen). cDNA was obtained by using Superscript RNaseH$^-$ reverse transcriptase (Invitrogen). All cDNAs were normalized to the β-actin reverse transcription-PCR (RT-PCR) product. Standard RT-PCR for EGFRvIII was done as described in ref. 29.

Fluorescence-activated cell sorting

Following enzymatic and mechanical dissociation, cells from primary GBM tissues and from experimental xenografts were stained with rabbit antihuman EGFR (clone EGFR.1, AbD Serotec), rat antihuman CD34/CD45/CD11b (Becton Dickinson), antihuman AC133 (Miltenyi), mouse anti-CD15 (clone MMA, Becton Dickinson), and antihuman pan-HLA (Becton Dickinson). Cells were sorted on a Becton Dickinson FACSVantage SE FACSDiVa. The purity of each cell fraction ranged between 90% and 99%. Fluorescence-activated cell sorting (FACS) analysis of CSC lines was done as described above, without enzymatic digestion.

Culture propagation, population analysis, and cloning

Established GBM CSCs were cultured as previously described (27).

Microarray-based gene expression profiling

See Supplementary Experimental Procedure for details.

Evaluation of CSC tumorigenicity by orthotopic implantation

Tumorigenicity was determined by injecting all the distinct cell preparations orthotopically in *nu/nu* mice (27). Magnetic resonance imaging (MRI) analysis was performed as described in Supplementary Experimental Procedure.

Immunofluorescence analysis was performed on cryostat sections using mouse monoclonal antihuman EGFR (1:100; Calbiochem). Details can be found in Supplementary Data.

Western blotting

Lysates from GBM tissues and CSCs were immunoblotted according to standard protocols. The primary antibodies used were rabbit anti-EGFR, rabbit anti–phosphorylated EGFR (Tyr^{1068}; Cell Signaling), rabbit anti-ErbB2 (Calbiochem) and rabbit anti-Erbb3 (Santa Cruz Biotechnology), rabbit anti–phosphorylated mitogen-activated protein kinase (MAPK; Cell Signaling), and rabbit anti–phosphorylated Akt (Ser^{473}; Cell Signaling). As a loading control, a mouse anti–β-tubulin antibody was used (Sigma-Aldrich).

Lentiviral vector generation, production, and cell infection

Human wild-type (wt) EGFR cDNA (Upstate) was cloned into the monocistronic transfer lentiviral vector pCCL.sin.cPPT.PGK.GFP.WPRE11. CSCs were transduced with 1×10^7 transduction units/mL of lentiviral vectors for 16 hours.

Lentiviral vectors coding for shRNAs targeted against the human EGFR were purchased from Sigma (Mission RNAi). Infection of CSCs was performed according to the manufacturer's instructions.

Immunofluorescence and fluorescence *in situ* hybridization

Immunofluorescence was performed as described in ref. 27, using mouse antihuman EGFR (Calbiochem) and rabbit polyclonal anti-GFP (Molecular Probes). Fluorescence *in situ* hybridization (FISH) was performed using the kit from Dako, according to the manufacturer's instructions. Filamentous actin (F-actin) was stained by TRITC-conjugated phalloidin (Chemicon).

Pharmacologic EGFR inhibition in CSCs

AG1478 (Calbiochem) was used at the indicated final concentrations in complete medium. DMSO was used at the same concentration as the vehicle control. Cell proliferation was measured by an MTT incorporation assay.

Invasion assays

Invasion assays were performed in Matrigel-coated 8-μm-pore Transwell chambers (Corning Costar). EGFR^{pos} and EGFR^{neg} CSCs were seeded in sister cultures on the upper side of the chambers in complete medium and allowed to migrate for 5 and 7 days, respectively, with or without AG1478. Noninvaded cells on the upper side of the filters were or were not scraped off, and those that migrated to the lower side were fixed and stained by using DiffQuick (Dade Behring). The extent of cell migration was normalized

Published OnlineFirst September 21, 2010; DOI:10.1158/0008-5472.CAN-10-2353

to the total number of viable cells in the corresponding unscraped culture.

Results

EGFR expression identifies distinct cell subpopulations within human primary GBM and GBM CSC lines

Several GBM surgical specimens were tested for EGFR mRNA expression by both microarrays and semiquantitative RT-PCR and all were shown to express the transcript (Table 1). However, immunohistochemistry on corresponding paraffin-embedded sections showed that, in agreement with the literature, only 50% of specimens were characterized by diffuse EGFR staining, which was particularly intense in small-sized round tumor cells ($EGFR^{pos}$ tumor samples; Fig. 1A, Supplementary Fig. S1). Accordingly, the other specimens displayed negligible EGFR expression that was restricted mostly to tumor-infiltrating inflammatory cells ($EGFR^{neg}$ tumor samples; Fig. 1A). Western blotting (WB) analysis confirmed the immunohistochemistry findings (Fig. 1B). Hence, EGFR protein distribution identifies two main distinct subtypes of human GBM (16).

By FISH, a subset of $EGFR^{pos}$ tumor specimens showed *EGFR* gene amplification and expression of mutant EGFRvIII that, in some patients, correlated with EGFR protein levels (Fig. 1C and D; Table 1). Interestingly, $EGFR^{pos}$ tumors contained small and thin CD31-positive vessels (Fig. 1E), whereas $EGFR^{neg}$ tumors were characterized by an actively proliferating vasculature [mean vessel area (±SEM), 853.1 ± 214.1 and 2,500.2 ± 615.1 μm^2 in $EGFR^{pos}$ and $EGFR^{neg}$ GBMs, respectively; $P > 0.05$, Student's t test; $n = 7$; Fig. 1E]. All specimens expressed similar levels of stem cell–associated proteins, such as Sox2 and BMI1 (Fig. 1F), and of glial fibrillary acidic protein (GFAP; data not shown).

Interestingly, whereas immunohistochemistry indicated that EGFR was expressed in the totality of GBM cells, flow cytometry suggested that EGFR expression could be retrieved only in a smaller proportion of cells. Of note, within this $EGFR^{pos}$ cell fraction, a conspicuous subset of cells colabeled with the endothelial marker CD34 and the hematopoietic markers CD45 and CD11b (Fig. 1G), indicating that they were stromal cells. The CSC marker CD133 (30) was more expressed in proper tumor cells than in stromal cells in $EGFR^{pos}$ tumors, whereas the opposite was detected in $EGFR^{neg}$ tumors. On the contrary, CD15 was always more expressed in the stromal cell compartment in both $EGFR^{pos}$ and $EGFR^{neg}$ tumors (refs. 31, 32; Supplementary Table S1).

Thus, the frequency of $EGFR^{pos}$ proper tumor cells in GBM, calculated after the exclusion of stromal cells, ranged from 0% to 35% of the total tumor cell number (Table 1). Of note, some $EGFR^{pos}$ proper tumor cells also labeled with AC133 and/or CD15 markers, whereas $EGFR^{neg}$ cells did not (Fig. 1F and H; Supplementary Table S2).

To formally show that EGFR might also play a role in the biology of GBM CSCs *in vitro*, we tested 13 GBM CSC lines previously validated for being bona fide CSC lines (Supplementary Fig. S2). All CSC lines expressed EGFR mRNA, whereas only 5 of 13 CSC lines also expressed the EGFR protein (Table 2). Among the $EGFR^{pos}$ CSC lines, only 6% to 70% of cells expressed the receptor, suggesting that multiple GBM subpopulations could also be identified based on EGFR expression in CSC lines.

Interestingly, many $EGFR^{pos}$ and $EGFR^{neg}$ CSC lines contained $AC133^{pos}$ and $CD15^{pos}$ cells (Table 2; Supplementary Table S3). However, one of five $EGFR^{pos}$ CSC lines and four of eight $EGFR^{neg}$ CSC lines did not contain any $AC133^{pos}$ and $CD15^{pos}$ cells at all.

EGFR expression identifies GBM subpopulations with a distinctive gene signature

To molecularly analyze the above-described GBM subpopulations, we purified them from (*a*) $EGFR^{pos}$ single patients' tumor specimens, (*b*) $EGFR^{neg}$ specimens, and (*c*) $EGFR^{pos}$ CSC lines.

$EGFR^{pos}$ patient samples T1224, T0131, T0222, and T0321 contained (*a*) $EGFR^{pos}/AC133^{neg}$ cells (region R1), (*b*) $EGFR^{pos}/AC133^{pos}$ cells (R2), and (*c*) $EGFR^{neg}/AC133^{neg}$ (R3) cells. Two of them also contained a small proportion of $EGFR^{pos}/CD15^{pos}$ cells (Fig. 2A and B; Supplementary Table S2). Stromal cells were excluded from sorting.

Immediately after cell sorting and purity assessment, without any *in vitro* manipulation, the different GBM fractions were subjected to transcriptional profiling by whole-transcript microarrays (Fig. 2C). $EGFR^{pos}$ cell subpopulations displayed a specific molecular signature clearly distinguishable from that of double-negative cells (R3). Of note, a subset of 163 genes was differentially expressed between $EGFR^{pos}$ and $EGFR^{neg}$ cell subpopulations, even when isolated from distinct patient specimens, suggesting that EGFR expression in GBM might affect common molecular determinants (Supplementary List S1). In addition to EGFR, the differentially expressed genes (DEG) upregulated in $EGFR^{pos}$ versus $EGFR^{neg}$ GBM fractions were related to biological processes such as tumor invasion and progression [e.g., periostin (*POSTN*), *LMO3*, and *AQP4*]. Conversely, genes overexpressed in $EGFR^{neg}$ GBM fractions were mostly involved in the interaction of tumor cells with the microenvironment [e.g., *PDGFRB, Notch3, PTPRK*, lumican (*LUM*), and endothelin receptor A (*EDNRA*)]. Thus, GBMs contain molecularly distinct subpopulations of tumor cells.

When the same freshly isolated cell fractions were cultured *in vitro* by the NeuroSphere Assay under limiting dilution conditions (33), $EGFR^{pos}$ cell fractions gave rise to a higher frequency of secondary neurospheres than $EGFR^{neg}$ cells (Fig. 2D).

Cell subpopulations expressing different levels of EGFR were also purified from $EGFR^{pos}$ CSC lines (Fig. 2E–G). Immediately after sorting, $EGFR^{high}$ (R4), $EGFR^{low}$ (R5), and $EGFR^{neg}$ (R6) CSC subpopulations were validated by WB (Fig. 2H) and subjected to transcriptional profiling, which indicated that each subpopulation was molecularly distinct from the others (Fig. 2I; Supplementary List S2). Of note, genes upregulated in $EGFR^{high}$ and $EGFR^{low}$ versus $EGFR^{neg}$ fractions were also highly expressed in the most malignant

Published OnlineFirst September 21, 2010; DOI:10.1158/0008-5472.CAN-10-2353

Table 1. EGFR expression in GBM patients' tumor specimens

Patient code	WHO tumor stage	Age/sex	EGFR wt mRNA	EGFR vIII mRNA	*EGFR* gene amplification	EGFR protein expression (% of positive cells)	EGFR protein expression (membrane staining intensity)
$EGFR^{pos}$ GBMs							
T0131	IV	58/M	2+	0	High amplification	70–90	3+
T0222	IV	57/F	2+	1+	High amplification	80–100	3+
T1210	IV	56/M	2+	0	High amplification	80–100	3+
T1224	IV	59/M	2+	1+	High amplification	70–90	3+
T0418	IV	63/M	1+	0	High polysomy	70–90	2+
T0625	IV	74/F	1+	0	Low amplification	70–90	2+
T0321	IV	59/M	2+	1+	High amplification	70–90	3+
$EGFR^{neg}$ GBMs							
T0104	IV	49/M	1+	0	No amplification	10–20	1+
T0109	IV	47/M	1+	0	No amplification	10–20	1+
T0125	IV	49/M	1+	0	No amplification	10–20	1+
T0130	IV	72/F	1+	0	No amplification	15–25	1+
T0325	IV	51/M	1+	0	No amplification	0	0
T0512	IV	75/F	1+	0	No amplification	5–10	1+
T1003	IV	65/M	1+	0	No amplification	5–10	1+

Patient code	Total $EGFR^{pos}$ cells (%)	$EGFR^{pos}$ tumor cells (%)	$EGFR^{pos}$ stromal cells (%)
$EGFR^{positive}$ GBMs			
T0131	20.8	4.0	16.8
T0222	76.8	35.2	41.6
T1210	13.7	10.7	3.0
T1224	78.1	20.3	57.8
T0418	36.6	12.4	24.2
T0625	22.4	8.9	13.5
T0321	39.1	21.7	17.4
$EGFR^{negative}$ GBMs			
T0104	4.9	0.9	4.0
T0109	17.3	0.0	17.3
T0125	19.0	1.6	17.4
T0130	25.3	3.3	22.0
T0325	0.0	0.0	0.0
T0512	4.4	0.0	4.4
T1003	7.5	0.0	7.5

NOTE: FISH scores: high gene amplification, >10 gene copies in >10% of the cells; low gene amplification, 6 to 10 gene copies in >10% of the cells; high polysomy, >4 gene copies in >40% of the cells; low polysomy, >4 gene copies in >10% but <40% of the cells; no amplification, 1 to 4 gene copies. Immunohistochemistry scores: 3+, very intense membrane staining; 2+, intense membrane staining; 1+, moderate staining; 0, no staining.

molecular subclasses of primary GBM (i.e., the proliferative and mesenchymal subtypes, as identified in refs. 21 and 34; Supplementary Fig. S3). Likewise, genes downregulated in $EGFR^{pos}$ fractions were also downregulated in the same malignant molecular subtypes.

As shown by clonogenic assays performed under limiting dilution conditions and by long-term population analysis, $EGFR^{low}$ and $EGFR^{neg}$ cell fractions displayed the highest proliferative capacity, whereas $EGFR^{high}$ cell subpopulations showed a transiently reduced growth ability that required a few subculturing passages to be completely restored to the presorting levels (Fig. 2J). All subpopulations contained the same percentage of Bmi1- and Sox2-expressing cells, which was not affected by cell differentiation (Supplementary Fig. S4).

When tested immediately after sorting, $EGFR^{high}$ and $EGFR^{low}$ fractions contained 100% of $EGFR^{pos}$ cells, whereas $EGFR^{neg}$ fractions were devoid of any $EGFR^{pos}$ cells (Fig. 2K). However, after several subculturing passages, each cell

Published OnlineFirst September 21, 2010; DOI:10.1158/0008-5472.CAN-10-2353

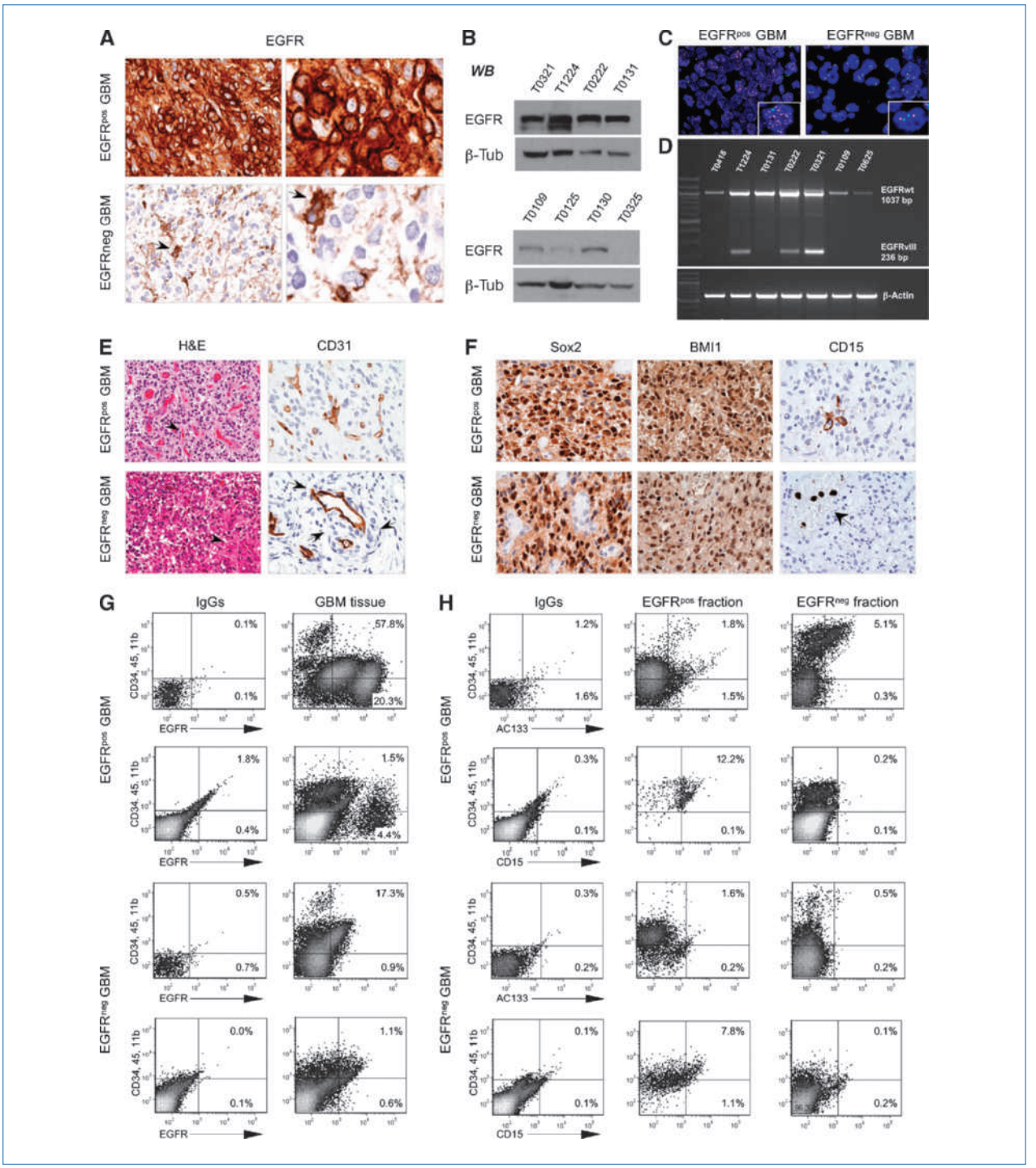

Figure 1. EGFR expression identifies distinct cell subpopulations within primary human GBM. A, $EGFR^{pos}$ GBM tumors show diffuse and intense reactivity for EGFR in small and round neoplastic cells (T1224). $EGFR^{neg}$ GBM specimens show EGFR staining restricted to tumor-infiltrating inflammatory cells (black arrow; T0109). Magnification, ×400 and ×800. B, WB confirms EGFR protein levels in GBM patients' specimens. C, FISH analysis indicates that the *EGFR* gene is amplified only in $EGFR^{pos}$ tumors. D, the mutant EGFRvIII can be detected in a subset of $EGFR^{pos}$ tumors by RT-PCR. E, $EGFR^{pos}$ tumors contain modestly proliferating vessels (arrows), whereas $EGFR^{neg}$ tumors show an enlarged and proliferating vasculature (arrows). H&E and CD31 staining; magnification, ×200 and ×400. F, $EGFR^{pos}$ and $EGFR^{neg}$ tumors contain similar numbers of Sox2 and $Bmi1^{pos}$ cells. $CD15^{pos}$ proper tumor cells can be detected only in $EGFR^{pos}$ (arrow at bottom right, $CD15^{pos}$ monocytes within a vessel). Magnification, ×400. G, in $EGFR^{pos}$ tumors, many $EGFR^{pos}$ cells are proper tumor cells, whereas in $EGFR^{neg}$ tumors the few $EGFR^{pos}$ cells are stromal/inflammatory cells. H, the $EGFR^{pos}$ fractions from $EGFR^{pos}$ specimens contain $AC133^{pos}$ and $CD15^{pos}$ cells (top middle), which are either tumor cells or stromal cells. On the contrary, $EGFR^{neg}$ fractions (top right) and $EGFR^{neg}$ GBM tumors (bottom) contain only stromal $AC133^{pos}$ and $CD15^{pos}$ cells.

Published OnlineFirst September 21, 2010; DOI:10.1158/0008-5472.CAN-10-2353

Table 2. Characterization of EGFR^{pos} and EGFR^{neg} GBM CSC lines for their expression of the putative CSC enrichment markers AC133 and CD15

CSC line code	EGFR wt mRNA	EGFR vIII mRNA	*EGFR* gene amplification (FISH)	PTEN expression (WB)	EGFR^{pos} cells (%)	AC133^{pos} cells (%)	CD15^{pos} cells (%)
EGFR^{positive} CSC lines							
L0627	2+	0	High amplification	2+	25.8 ± 3.5	42.9 ± 15.2	22.3 ± 2.9
L0804	2+	0	High polysomy	0	7.7 ± 1.2	5.9 ± 0.9	2.7 ± 1.0
L0306	2+	0	Low amplification	3+	21.1 ± 3.0	0.0	28.1 ± 2.9
L0201	2+	0	High polysomy	1+	79.1 ± 3.9	3.1 ± 1.5	13.7 ± 0.9
L0605	2+	0	Low polysomy	0	8.5 ± 2.8	0.0	0.0
EGFR^{negative} CSC lines							
L0104	1+	0	No amplification	0	2.0 ± 0.8	30.1 ± 13.8	50.8 ± 3.2
L0223	1+	0	No amplification	3+	0.0	0.0	10.7 ± 1.3
L0125	1+	0	No amplification	1+	0.0	0.0	0.0
L1210	1+	0	No amplification	0	2.4 ± 1.2	0.0	0.0
L0314	1+	0	No amplification	3+	0.0	0.0	5.9 ± 1.7
L0325	1+	0	No amplification	0	0.0	0.0	0.0
L0512	1+	0	No amplification	3+	1.7 ± 0.6	2.1 ± 1.4	11.7 ± 2.9
L0418	1+	0	No amplification	0	0.0	18.2 ± 4.5	0.0

NOTE: EGFR wt and EGFRvIII mRNA levels were measured by semiquantitative RT-PCR. EGFR, AC133, and CD15 expression was measured by flow cytometry. High gene amplification, >10 gene copies in >10% of the cells; low gene amplification, 6 to 10 gene copies in >10% of the cells; high polysomy, >4 gene copies in >40% of the cells; low polysomy, >4 gene copies in >10% but <40% of the cells; no amplification, 1 to 4 gene copies. The frequency of EGFR^{pos} cells within EGFR^{pos} CSC lines remained stable throughout extensive subculturing. Likewise, EGFR^{neg} CSC lines were never shown to comprise EGFR^{pos} cells even at very high subculturing passages.

fraction regenerated the same frequency of EGFR^{pos} and EGFR^{neg} cells found in the parental bulk population, recapitulating the original cellular heterogeneity (Fig. 2K).

EGFR expression confers increased tumorigenic capacity to GBM cells

To assess whether EGFR expression might affect the tumorigenic ability of GBM cells, R1, R2, and R3 fractions, purified from EGFR^{pos} GBM specimens, were transplanted into the brain of *nu/nu* mice, without any prior *in vitro* manipulation (Fig. 3A; Supplementary Fig. S1). MRI-based volumetric analysis showed that EGFR^{pos} cells were characterized by enhanced tumorigenic capacity (Fig. 3A). However, EGFR^{neg}/AC133^{neg} cells were also capable of initiating tumors, although these developed significantly more slowly than those generated by EGFR^{pos} GBM cells (Kaplan-Meier analysis; Fig. 3B).

Notably, EGFR expression was retrieved not only in xenografts derived from EGFR^{pos} cells but also in those derived from EGFR^{neg} fractions (Fig. 3C–E). Importantly, the latter xenografts never contained either AC133^{pos} cells (Fig. 3E) or CD15^{pos} cells (Fig. 3F, Supplementary Fig. S1). Thus, as recently shown for other stem cell markers in melanoma (35), EGFR expression in GBM TICs is dynamically regulated, given that EGFR^{neg} cells can become EGFR^{pos} on transplantation. Most importantly, EGFR expression positively correlates with gliomagenesis.

Although R1-, R2-, and R3-derived xenografts showed the same expression of SOX2 and Bmi1 (Fig. 3G and data not shown), they were molecularly different (Fig. 3H). By microarray-based analysis, proinvasive genes were overexpressed in EGFR^{pos} cell–derived xenografts, whereas genes involved in angiogenesis were upregulated in EGFR^{neg} cell–derived xenografts (Supplementary Fig. S5).

In agreement with these latter findings and with molecular data obtained on EGFR^{pos} and EGFR^{neg} subpopulations (Fig. 2C), xenografts from EGFR^{pos} cells were shown to be highly invasive, with cells spreading preferentially along the gray matter while avoiding white matter fiber tracts (Fig. 3C and G; Supplementary Figs. S1 and S6). On the contrary, tumors formed by EGFR^{neg} cells showed well-demarcated boundaries, with cells migrating preferentially along white matter tracts (Fig. 3C and G; Supplementary Figs. S1 and S6). Accordingly, EGFR^{pos} cell–induced xenografts were characterized by thin, regularly shaped blood vessels and a low proliferative index, whereas tumors from EGFR^{neg} cells contained enlarged and proliferating vessels and a higher frequency of mitotic cells (Supplementary Figs. S1 and S6).

Thus, EGFR expression confers different invasive, angiogenic, and tumorigenic abilities to GBM cells *in vivo*.

Notably, the same functional differences observed between xenografts generated by EGFR^{pos} and EGFR^{neg} TICs purified from GBM specimens could also be detected in xenografts

Published OnlineFirst September 21, 2010; DOI:10.1158/0008-5472.CAN-10-2353

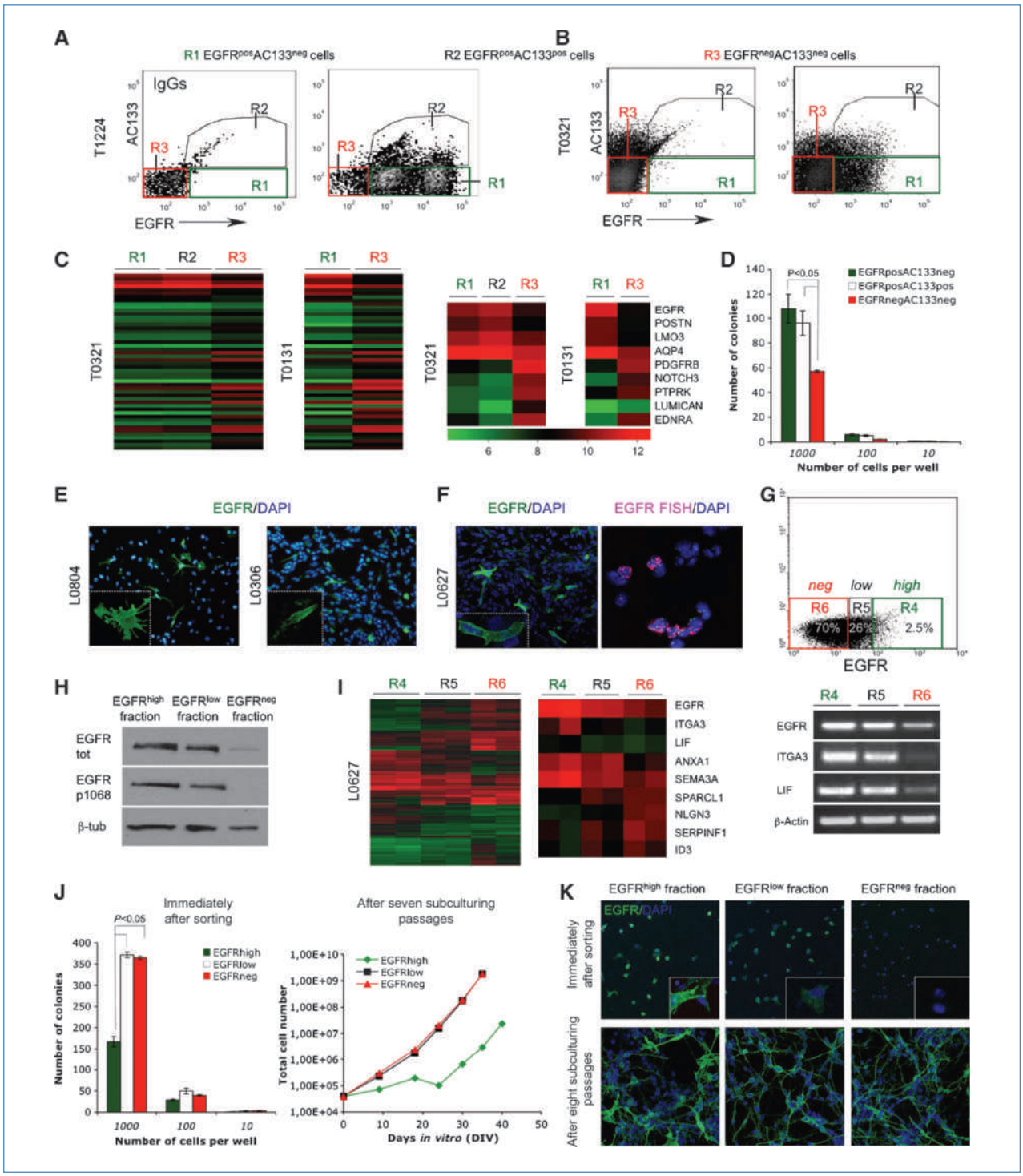

Figure 2. EGFR expression identifies GBM subpopulations with distinctive gene signatures and different growth characteristics *in vitro*. A and B, $EGFR^{pos}/AC133^{neg}$ (R1), $EGFR^{pos}/AC133^{pos}$ (R2), and $EGFR^{neg}/AC133^{neg}$ (R3) cells were isolated from $EGFR^{pos}$ tumor specimens by FACS (IgGs, isotype controls). C, global gene expression data in R1, R2, and R3 fractions purified from patients' specimens (left). The expression of a selection of coregulated genes is highlighted in the heatmaps (right). D, limiting dilution clonogenic assay of R1, R2, and R3 fractions immediately after sorting. E, different CSC lines comprise variable amounts of $EGFR^{pos}$ cells. Magnification, ×200 (insets, ×600). F, some $EGFR^{pos}$ CSCs display *EGFR* gene amplification. G, different CSC subpopulations could be isolated by FACS from $EGFR^{pos}$ CSC lines based on their EGFR expression (region R4, $EGFR^{high}$ CSCs; R5, $EGFR^{low}$ CSCs; R6, $EGFR^{neg}$ CSCs; L0627). H, WB analysis shows that EGFR is activated in $EGFR^{high}$ and $EGFR^{low}$ CSCs but is absent in $EGFR^{neg}$ CSCs. I, global gene expression data of R4, R5, and R6 GBM fractions purified from $EGFR^{pos}$ CSC lines. Semiquantitative RT-PCR validation of DEGs. J, clonogenic assay and long-term growth curves of R4, R5, and R6 CSCs immediately after sorting and after *in vitro* culture. K, EGFR expression in CSC fractions immediately after sorting (top) and on *in vitro* culture (bottom; EGFR, green; magnification, ×200).

Published OnlineFirst September 21, 2010; DOI:10.1158/0008-5472.CAN-10-2353

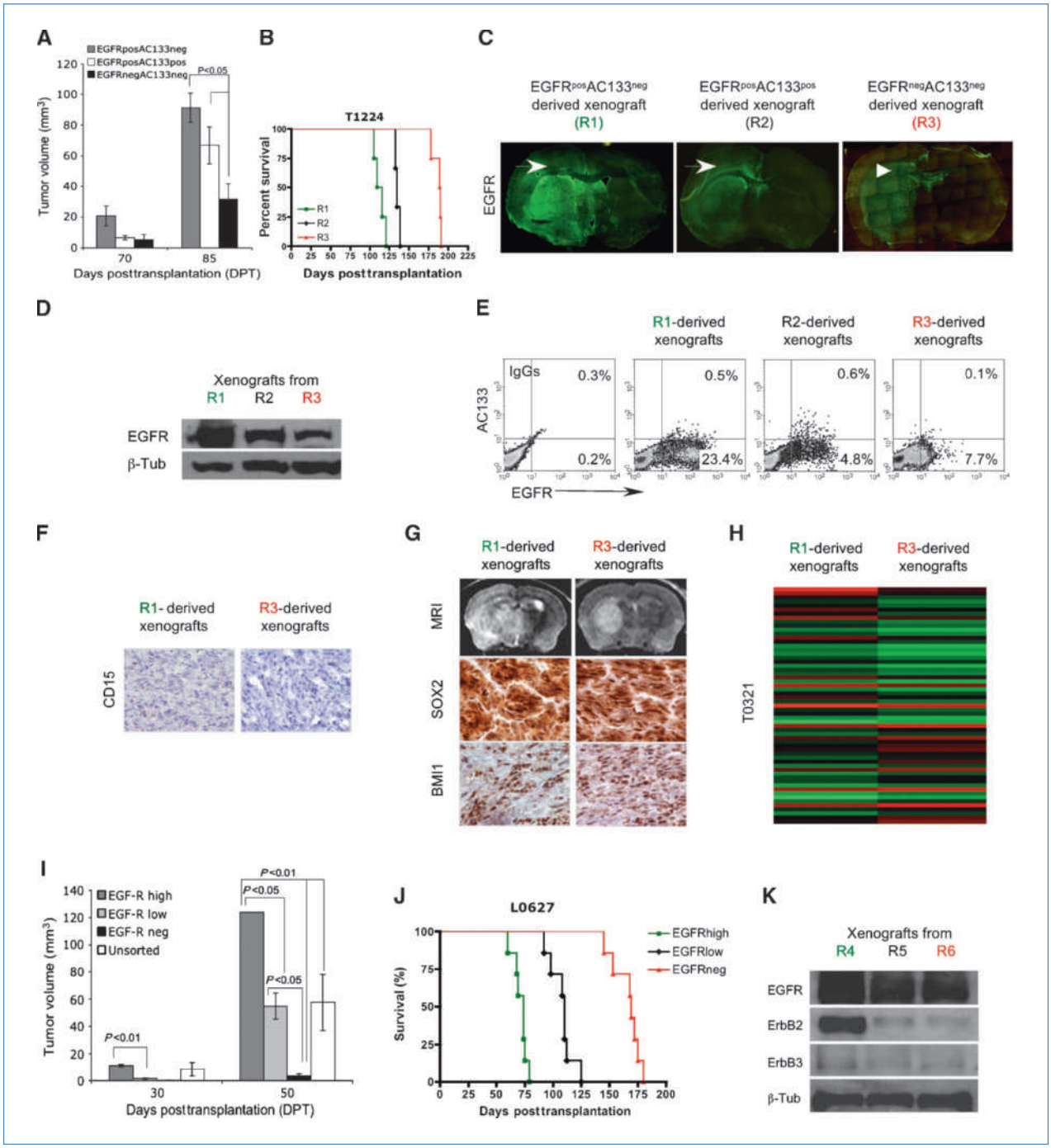

Figure 3. EGFR expression identifies TICs with different tumorigenic capacities. A, $EGFR^{pos}$ cell–derived tumors, independently of the coexpression of AC133, were significantly larger than tumors induced from $EGFR^{neg}AC133^{neg}$ cells. $P < 0.05$, one-way ANOVA with Bonferroni test ($n = 5$, six independent experiments). B, Kaplan-Meier survival curves ($P < 0.01$). C, EGFR expression detected by an antihuman EGFR is retrieved in all xenografts, including $EGFR^{neg}AC133^{neg}$ cell–derived tumors (EGFR, green). $EGFR^{pos}$ cell–derived tumors are characterized by an infiltrative pattern of growth. Tumor cells disperse within the gray matter, avoiding the corpus callosum (white arrow). $EGFR^{neg}AC133^{neg}$ cells give rise to expanding tumors, mostly confined within the injection site, which migrate and invade along white matter tracts (white arrowhead). D, WB confirms EGFR protein expression in all xenografts. E, the same distinct $EGFR^{pos}$ and $EGFR^{neg}$ subpopulations as detected in the parental tumor were retrieved in the corresponding xenografts by flow cytometry. $CD15^{pos}$ cells (F) were not retrieved in any xenografts by immunohistochemistry. G, a similar frequency of Sox2 and Bmi1 immunoreactive cells could be retrieved in R1- and R3-derived xenografts. H, global gene expression data of R1- and R3-derived xenografts. I to J, EGFR expression confers enhanced tumorigenic potential to $EGFR^{pos}$ fractions from $EGFR^{pos}$ CSC lines (one-way ANOVA with Bonferroni test, $n = 5$, three independent experiments). $P < 0.01$, Kaplan-Meier survival curves. K, EGFR expression was retrieved in all xenografts, whereas ErbB2 was highly expressed only in $EGFR^{high}$ CSC–derived tumors (WB).

Published OnlineFirst September 21, 2010; DOI:10.1158/0008-5472.CAN-10-2353

generated by *in vitro* expanded $EGFR^{pos}$ and $EGFR^{neg}$ CSC lines (Supplementary Fig. S2; ref. 36).

Because EGFR expression in $EGFR^{neg}$ cell–derived xenografts might be due to contaminating $EGFR^{pos}$ tumor cells, we purified $EGFR^{neg}$ tumor cells from $EGFR^{neg}$ specimens that were totally devoid of $EGFR^{pos}$, $AC133^{pos}$, and $CD15^{pos}$ proper tumor cells (Fig. 1A, G, and H; Supplementary Table S1). FACS-purified $EGFR^{neg}/AC133^{neg}$ cells generated xenografts that expressed EGFR but were negative for AC133 and CD15, thus confirming that EGFR might indeed play a prominent role in glioma formation (Supplementary Fig. S7). Notably, both *in vivo* limiting dilution analysis and serial transplantation proved that all GBM subpopulations identified based on EGFR expression could be considered bona fide TICs (Supplementary Fig. S8).

The tumorigenic potential of $EGFR^{high}$, $EGFR^{low}$, and $EGFR^{neg}$ cells purified from different $EGFR^{pos}$ CSC lines (Figs. 2G and 3I and J and Supplementary Fig. S9 for L0627 and Supplementary Fig. S9 for L0605) was also tested. As observed for xenografts obtained from GBM specimen–derived subpopulations (Fig. 3A–E), tumors derived from $EGFR^{high}$ and $EGFR^{low}$ CSCs were larger than those generated from $EGFR^{neg}$ cell fractions, which, again, displayed tumor-initiating ability (Fig. 3I and J). Again, $EGFR^{neg}$ CSC fraction–derived tumors expressed EGFR, confirming that EGFR upregulation occurred during experimental tumorigenesis (Fig. 3K). ErbB2 expression was detected only in $EGFR^{high}$ cell–derived tumors, suggesting that the xenografts were molecularly heterogeneous (Fig. 3K).

To understand the relationship between the expression of EGFR and that of the CSC markers CD15 and AC133 in terms of tumor-initiating potential, $EGFR^{pos}CD15^{neg}$ (R4), $EGFR^{pos}CD15^{pos}$ (R5), $EGFR^{neg}CD15^{pos}$ (R6), and $EGFR^{neg}CD15^{neg}$ (R7) as well as $EGFR^{pos}CD15^{neg}AC133^{neg}$ (R1) and $EGFR^{neg}CD15^{neg}AC133^{neg}$ (R3) fractions were purified from L0627 and L0605 (Supplementary Fig. S9). Interestingly, $EGFR^{pos}$ subpopulations, independent of the coexpression of AC133 and/or CD15, generated tumors that developed much earlier and grew larger than those generated by $EGFR^{neg}$ fractions. Consistent with previous findings, CSC lines/subpopulations negative for EGFR, AC133, and CD15 generated xenografts that did not express either of the two markers *in vivo* but did express the EGFR (Supplementary Figs. S2 and S9).

Thus, all of our GBM CSC lines, taken as a whole or fractionated into subpopulations and independent of their basal EGFR expression, gave rise to xenografts that upregulated the EGFR significantly (Fig. 3K; Supplementary Figs. S2 and S9). To understand the mechanism underlying EGFR expression in $EGFR^{neg}$ cell–derived xenografts, we hypothesized that because $EGFR^{neg}$ GBM cells retain EGFR transcript expression (Tables 1 and 2; Fig. 2C and I), *in vivo* EGFR expression might be regulated posttranscriptionally. Indeed, when we simulated *in vitro* the mitogen-reduced adult brain microenvironment by starvation, $EGFR^{neg}$ CSCs efficiently reexpressed the EGFR protein (Supplementary Fig. S2). Accordingly, when the same CSCs were reexposed to standard mitogen concentrations, they downregulated EGFR expression, as may occur *in vivo* during tumor progression when tumor-infiltrating stromal cells secrete mitogens in a paracrine fashion (37).

Enforced EGFR expression by gene transfer increases the malignant behavior of CSCs *in vitro* and *in vivo*

Lentiviral vector–mediated EGFR expression in three distinct $EGFR^{neg}$ CSC lines allowed the expression of a fully functional receptor (Fig. 4A). Of note, the majority of EGFR-transduced cells acquired a fibroblastoid shape and developed stress fibers and actin-driven lamellipodia, all known markers of epithelial-mesenchymal transition and enhanced malignancy (Fig. 4B; Supplementary Table S4). Consistently, the average cell size was increased in most EGFR-transduced cells (Fig. 4C; Supplementary Table S4).

Gene expression profiling of naïve, mock, and EGFR-overexpressing CSC lines identified a common subset of DEGs that was altered in both L0104 and L0125 CSC lines, suggesting that enforced EGFR expression affected the same molecular determinants in different patient-derived CSC lines (Fig. 4D and E). In addition to *EGFR, LIF*, and *ITGA3*, genes previously shown to be also highly expressed in FACS-purified $EGFR^{pos}$ CSC fractions (Fig. 2I; Supplementary List S2), proinvasive genes such as *CXCL10* and *ICAM1* (38, 39) were upregulated in EGFR-transduced CSCs (Fig. 4D–E) and also overexpressed in the proliferative and mesenchymal subtypes of human GBM (ref. 2I; Supplementary Fig. S3). Accordingly, tumor suppressors such as *SPARCL1* (Fig. 2I), *ERBB4, ASCL1*, and *EDNRB*, which were downregulated in EGFR-transduced CSCs, were also downregulated in GBM malignant subtypes.

Notably, all EGFR-transduced CSC lines formed experimental tumors that were larger than those induced by the corresponding mock lines (Fig. 4F).

Genetic loss of function of EGFR reduces the malignancy of CSCs *in vitro* and *in vivo*

To silence EGFR expression stably, we exploited line L0201 and line L0627, which express high levels of EGFR in 70% and 30% of the cells, respectively (Table 2). The shRNA clones 204 and 206 induced EGFR protein knockdown with an efficiency of 60% and 70% in lines L0201 (Fig. 5A) and L0627 (data not shown), respectively. WB analysis confirmed the flow cytometry results and indicated an inhibition of downstream signaling pathways on EGFR silencing (Fig. 5B).

EGFR-knockdown CSCs displayed morphologic changes *in vitro*, with neurospheres appearing as well-differentiated cells (Fig. 5C). Consistently, the frequency of differentiated cells detected in shRNA-transduced CSCs increased under both proliferative (Fig. 5D) and differentiative culture conditions (data not shown).

Of note, tumors generated from EGFR-knockdown CSCs developed more slowly and were significantly smaller than those generated by the CTRL subclone, thus resulting in the increased survival of EGFR-knockdown CSC–transplanted mice (Fig. 5E).

Published OnlineFirst September 21, 2010; DOI:10.1158/0008-5472.CAN-10-2353

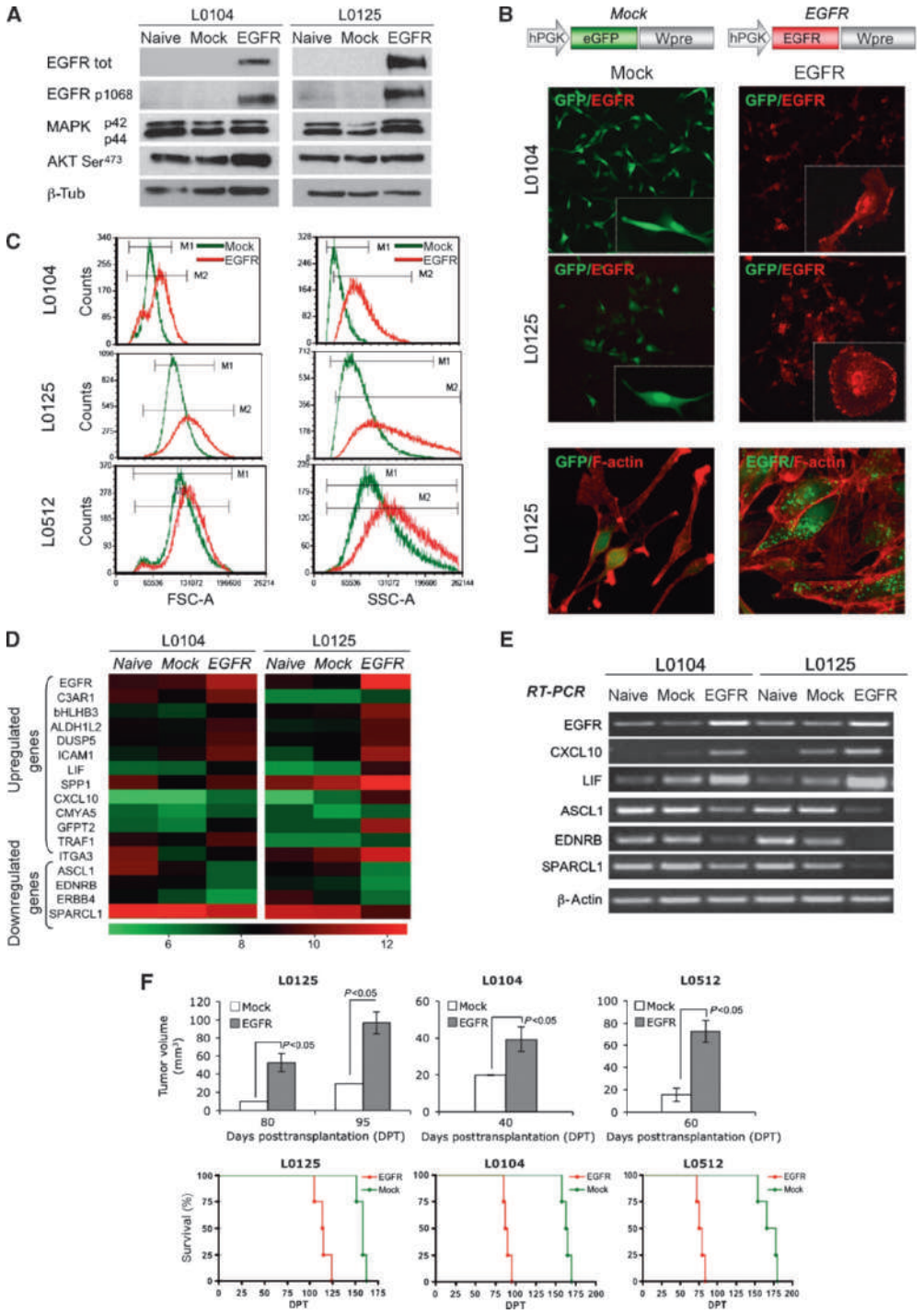

Figure 4. Overexpression of EGFR enhances the tumorigenic potential of CSCs. A, lentiviral-mediated *EGFR* gene transfer resulted in the expression of a functional EGFR, as indicated by phosphorylation at residue Tyr^{1068} and by the hyperactivation of downstream pathways. B, enforced EGFR expression in EGFR^{neg} CSCs (EGFR, red) correlates with changes in cell morphology, which are absent in GFP-transduced CSCs (GFP, green). F-actin staining (phalloidin, red). Magnifications: top, ×400; insets, ×1,000; bottom, ×1,000. C, EGFR overexpression in EGFR^{neg} CSCs induces a significant increase in their size. FSC-A and SSC-A. D, global gene expression data in naïve, mock-transduced, and EGFR-transduced CSC lines identify a subset of DEGs that are coregulated in different patient-derived CSC lines and modulated by enforced EGFR expression (*EGFR* gene signature). E, semiquantitative RT-PCR validation of DEGs. F, ectopic expression of EGFR in EGFR^{neg} CSC lines increases their tumorigenic potential and reduces mouse survival (Student's *t* test, $n = 5$, three independent experiments).

Published OnlineFirst September 21, 2010; DOI:10.1158/0008-5472.CAN-10-2353

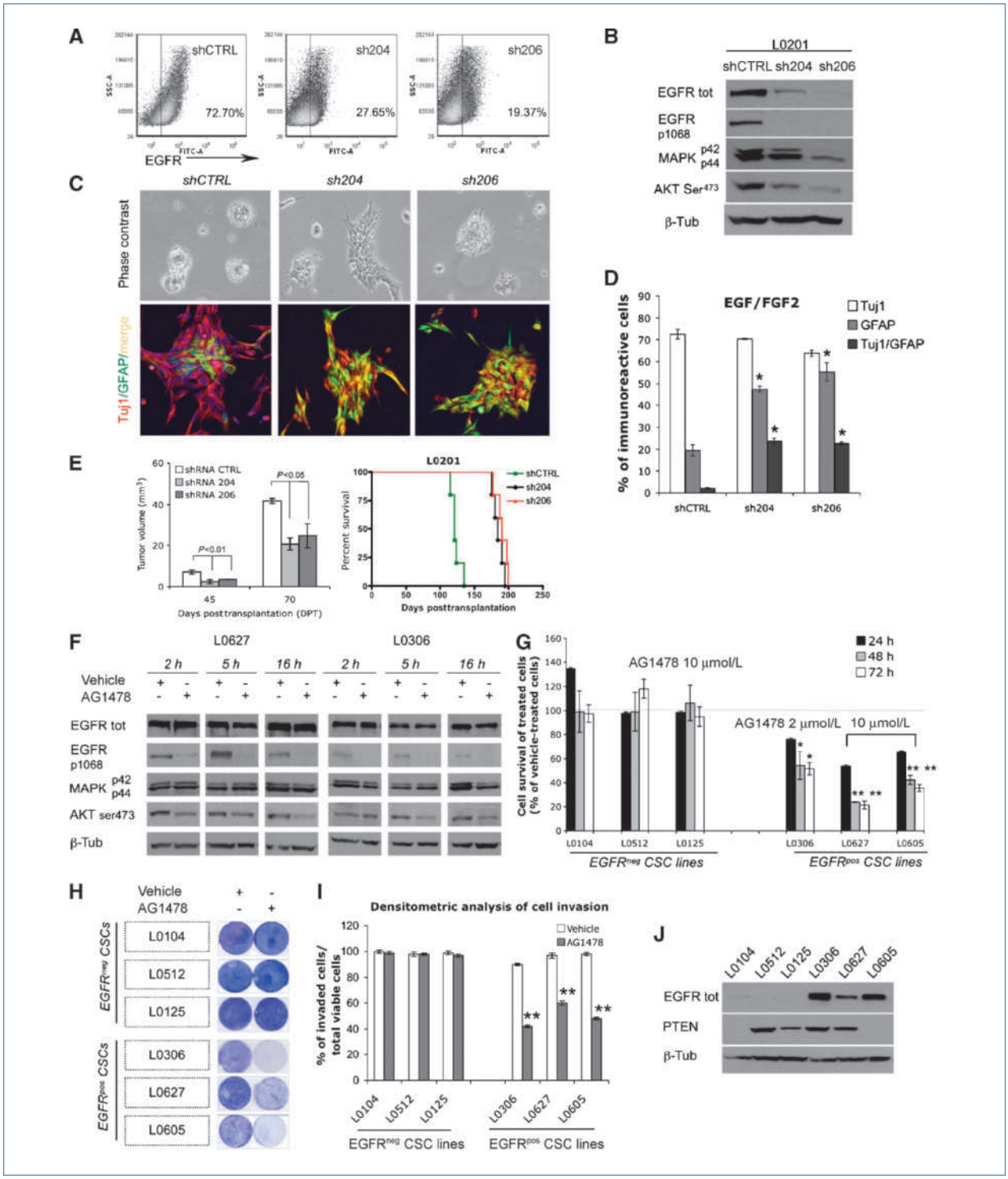

Figure 5. Inhibition of EGFR expression and activity negatively affects the malignant behavior of CSCs. A and B, flow cytometry and WB of L0201 shRNA 204 and shRNA 206 CSC subclones indicate efficient knockdown of EGFR protein and downregulation of MAPK and Akt downstream pathways. C and D, EGFR knockdown induces CSC differentiation. Tuj1, red; GFAP, green. Magnifications: top, ×200; bottom, ×400. *, $P > 0.05$, Student's t test. E, EGFR silencing in CSCs significantly decreases their tumorigenicity (one-way ANOVA with Bonferroni test, $n = 4$, two independent experiments). $P < 0.01$, Kaplan-Meier survival curves. F, AG1478 treatment inhibits the phosphorylation status of EGFR and Akt in CSCs (WB). G, $EGFR^{pos}$ CSC lines respond to treatment by decreasing their proliferation/survival, whereas $EGFR^{neg}$ CSC do not. *, $P > 0.05$; **, $P > 0.01$, Student's t test. H and I, EGFR inhibition by AG1478 negatively affects the invasive ability of CSCs. **, $P > 0.01$, Student's t test. J, CSC responsiveness to TKI is independent of PTEN expression (WB).

Published OnlineFirst September 21, 2010; DOI:10.1158/0008-5472.CAN-10-2353

EGFR^{pos} and EGFR^{neg} CSC lines differentially respond to pharmacologic inhibition of EGFR

To pharmacologically inhibit EGFR activity, we exploited the EGFR tyrosine kinase inhibitor (TKI) AG1478. WB analysis of two different EGFR^{pos} CSCs that were exposed to AG1478 for 2, 5, and 16 hours showed effective inhibition of EGFR autophosphorylation and a significant decrease in AKT phosphorylation, a hallmark of drug sensitivity (Fig. 5F).

Pharmacologic treatment of EGFR^{pos} CSC lines with AG1478 for up to 72 hours *in vitro* resulted in a significant decrease in CSC survival/proliferation (Fig. 5G). Relevantly, the survival and proliferation of EGFR^{neg} CSC lines were not affected by AG1478, even when the same lines were transduced with EGFR-coding vectors before treatment, suggesting that EGFR-overexpressing EGFR^{neg} CSC lines did not become addicted to EGFR (data not shown). Likewise, exposure of EGFR^{pos} CSCs to AG1478 strongly reduced their invasive capacity as compared with controls (Fig. 5H and I). Again, the invasive ability of EGFR^{neg} CSC lines was not affected by AG1478 exposure.

Interestingly, all the EGFR^{pos} CSC lines responded to pharmacologic treatment independently of the expression of PTEN, a putative molecular determinant of TKI responsiveness in patients with GBM (Fig. 5J; ref. 40).

Thus, EGFR^{pos} CSCs are responsive to pharmacologic inhibition by TKIs, whereas EGFR^{neg} CSCs are not.

Discussion

EGFR expression contributes to GBM heterogeneity

GBM is characterized by a high degree of heterogeneity, which is efficaciously reflected in the definition "multiforme." However, the intrinsic heterogeneity of GBM might refer not only to the well-known molecular diversity of GBM subtypes but also to the existence of genetically and functionally distinct cohorts of TICs within the same tumor.

In line with recent reports that provide new interpretations of the process of tumorigenesis in mouse hematopoietic malignancies (8), mouse colon cancer (41), human melanoma (10, 11), and brain tumors (42), our findings indicate that the initiation and progression of GBM may not depend on the presence of a single and rare fraction of CSCs, as proposed by the hierarchical model of tumor development (43). On the contrary, our data propose a different biological context, in which all GBM cells can be considered TICs with different degrees of stemness as proven by their different tumorigenic ability and by their distinct phenotypic and molecular features (44). In fact, all of our GBM-derived TIC subpopulations satisfy the requirements for bona fide CSCs: They self-renew *in vitro* and *in vivo* and give rise to experimental tumors that recapitulate the phenotypic traits of the tumor of origin under limiting dilution conditions and on serial transplantation.

Based on these observations, GBM tissue heterogeneity might be explained by the presence of a hierarchy of distinct TICs, as recently suggested for *in vitro* generated GBM CSC lines (13). These distinct TICs distribute along a gradient of tumorigenic potential that is strictly associated with EGFR expression.

Thus, our study provides conclusive evidence that the majority of GBM cells have tumorigenic capacity and that the hierarchical model of tumorigenesis might not fully apply to GBM.

Mechanisms underlying EGFR-dependent GBM heterogeneity

Tumor cells might modify their phenotype during tumor progression, with multiple cohorts of TICs being generated (45). In this study, we have shown that EGFR expression contributes to GBM cell diversity by generating different TIC populations. As to the mechanisms involved in the generation of EGFR-dependent phenotypic heterogeneity in GBM, the contribution of tumor microenvironment needs to be taken into consideration. Paracrine EGFR ligands, such as epidermal growth factor, are released by tumor stromal cells that, in this way, contribute to the activation of the EGFR signaling in both proper tumor cells and endothelial cells (37). When stroma-produced epidermal growth factor is secreted, EGFR protein downregulation occurs in target cells by receptor internalization, followed by lysosomal degradation.

In line with this view, it is tempting to speculate that the EGFR^{neg} cell component detected in EGFR^{pos} GBM might be generated from GBM cells that were originally EGFR^{pos} through receptor downregulation induced by excessive ligand stimulation during tumor progression, as we simulated *in vitro* by modulation of mitogen concentration. In addition, termination of EGFR signaling in EGFR^{neg} GBM cells might lead to the acquisition of compensatory additional genetic events, which might account for the molecular differences detected between EGFR^{pos} and EGFR^{neg} TICs. For instance, the expression of other receptor tyrosine kinases, such as PDGFRs, observed in EGFR^{neg} TIC fractions might contribute to their tumorigenic ability by synergizing with the EGFR re-upregulation required for experimental gliomagenesis. Indeed, PDGFR pathway activation has been recently shown to identify a GBM subtype that does not express the EGFR (46), thus suggesting that the latter GBM subtype might be sustained by EGFR^{neg} PDGFR^{pos} TICs.

EGFR^{pos} and EGFR^{neg} TICs can both give rise to experimental tumors that phenocopy the tumor of origin, and therefore, they both can be considered bona fide TICs. However, because EGFR^{pos} TICs are characterized by enhanced tumorigenic potential and highly invasive behavior, they might be envisioned as the "actual" GBM CSCs. Conversely, EGFR^{neg} TICs, which form tumors with low efficiency and need to re-upregulate the EGFR to be tumorigenic, might be better defined as "potential" GBM CSCs, which might be kept in a dormancy-like state by EGFR downregulation, being reactivated on exposure to appropriate stimuli when exposed to the *in vivo* microenvironment. In line with this notion, it has been recently shown that GBMs, which were EGFR^{neg} in origin, expressed the EGFR on recurrence (47).

Published OnlineFirst September 21, 2010; DOI:10.1158/0008-5472.CAN-10-2353

Therapeutic implications of EGFR-dependent GBM heterogeneity

The role of EGFR in the malignant progression of GBM and its effect on patient survival have been highly debated. Despite the controversial prognostic significance of EGFR expression in GBM, pharmacologic targeting of EGFR by means of TKIs has been proposed as a possible therapeutic strategy (40).

To date, single-agent EGFR inhibition in GBM did not achieve complete therapeutic efficacy. This failure has been ascribed primarily to the maintenance of a high level of Akt-dependent signaling in PTEN-mutated tumors (48) and to coactivation in the same tumor cell of multiple receptor tyrosine kinases, which might compensate for the effective inhibition of EGFR-dependent pathways (49).

By complementing these explanations, our findings suggest that the simultaneous presence of distinct TICs within the same tumor might also influence the outcome of EGFR-targeted therapies in GBM. Indeed, whereas effective inhibition of EGFR in our $EGFR^{pos}$ CSC lines can be achieved independently of PTEN expression, $EGFR^{neg}$ CSCs do not respond to treatment. By translating these results into a clinical perspective, in spite of the inhibition of the $EGFR^{pos}$ cell component in $EGFR^{pos}$ GBM, the nonresponsiveness of the $EGFR^{neg}$ TIC fraction to EGFR inhibitors might allow these cells to survive treatment and to support tumor relapse. Therefore, an effective therapeutic regimen should take into consideration the role of residual, nonresponder TICs. To this end, the development of a combination therapy targeted not only against the most aggressive "actual" TIC populations but also against the less malignant "potential" TICs will be necessary to improve the management of GBM.

Disclosure of Potential Conflicts of Interest

No potential conflicts of interest were disclosed.

Acknowledgments

We thank Alessio Palini and Chiara Villa for technical assistance with FACS. Antonella Iadanza for technical assistance with MRI, and Carol Stayton for editing of the manuscript.

Grant Support

Compagnia S. Paolo grants CSP-2002.0735 and CSP-2005.0153, the Oncology Research Programme-Istituto Superiore di Sanità, and the Fondazione Cariplo (R. Galli).

The costs of publication of this article were defrayed in part by the payment of page charges. This article must therefore be hereby marked *advertisement* in accordance with 18 U.S.C. Section 1734 solely to indicate this fact.

Received 06/28/2010; accepted 07/18/2010; published OnlineFirst 09/21/2010.

References

1. Bonnet D, Dick JE. Human acute myeloid leukemia is organized as a hierarchy that originates from a primitive hematopoietic cell. Nat Med 1997;3:730–7.
2. Vescovi AL, Galli R, Reynolds BA. Brain tumour stem cells. Nat Rev Cancer 2006;6:425–36.
3. Dick JE. Stem cell concepts renew cancer research. Blood 2008;112:4793–807.
4. Al-Hajj M, Wicha MS, Benito-Hernandez A, Morrison SJ, Clarke MF. Prospective identification of tumorigenic breast cancer cells. Proc Natl Acad Sci U S A 2003;100:3983–8, [erratum appears in Proc Natl Acad Sci U S A. 2003 May 27;100(11):6890].
5. Pece S, Tosoni D, Confalonieri S, et al. Biological and molecular heterogeneity of breast cancers correlates with their cancer stem cell content. Cell 2007;140:62–73.
6. Ricci-Vitiani L, Lombardi DG, Pilozzi E, et al. Identification and expansion of human colon-cancer-initiating cells. Nature 2007;445:111–5.
7. O'Brien CA, Pollett A, Gallinger S, Dick JE. A human colon cancer cell capable of initiating tumour growth in immunodeficient mice. Nature 2007;445:106–10.
8. Kelly PN, Dakic A, Adams JM, Nutt SL, Strasser A. Tumor growth need not be driven by rare cancer stem cells. Science 2007;317:337.
9. Adams JM, Strasser A. Is tumor growth sustained by rare cancer stem cells or dominant clones? Cancer Res 2008;68:4018–21.
10. Quintana E, Shackleton M, Sabel MS, Fullen DR, Johnson TM, Morrison SJ. Efficient tumour formation by single human melanoma cells. Nature 2008;456:593–8.
11. Held MA, Curley DP, Dankort D, McMahon M, Muthusamy V, Bosenberg MW. Characterization of melanoma cells capable of propagating tumors from a single cell. Cancer Res 2007;70:388–97.
12. Beier D, Hau P, Proescholdt M, et al. $CD133^{+}$ and $CD133^{-}$ glioblastoma-derived cancer stem cells show differential growth characteristics and molecular profiles. Cancer Res 2007;67:4010–5.
13. Chen R, Nishimura MC, Bumbaca SM, et al. A hierarchy of self-renewing tumor-initiating cell types in glioblastoma. Cancer Cell 2006;17:362–75.
14. Nicholas MK, Lukas RV, Jafri NF, Faoro L, Salgia R. Epidermal growth factor receptor-mediated signal transduction in the development and therapy of gliomas. Clin Cancer Res 2006;12:7261–70.
15. Benito R, Gil-Benso R, Quilis V, et al. Primary glioblastomas with and without EGFR amplification: relationship to genetic alterations and clinicopathological features. Neuropathology 2010;30:392–400.
16. Furnari FB, Fenton T, Bachoo RM, et al. Malignant astrocytic glioma: genetics, biology, and paths to treatment. Genes Dev 2007;21:2683–710.
17. Ohgaki H, Kleihues P. Population-based studies on incidence, survival rates, and genetic alterations in astrocytic and oligodendroglial gliomas. J Neuropathol Exp Neurol 2005;64:479–89.
18. Heimberger AB, Suki D, Yang D, Shi W, Aldape K. The natural history of EGFR and EGFRvIII in glioblastoma patients. J Transl Med 2005;3:38.
19. Layfield LJ, Willmore C, Tripp S, Jones C, Jensen RL. Epidermal growth factor receptor gene amplification and protein expression in glioblastoma multiforme: prognostic significance and relationship to other prognostic factors. Appl Immunohistochem Mol Morphol 2006;14:91–6.
20. Hoelzinger DB, Mariani L, Weis J, et al. Gene expression profile of glioblastoma multiforme invasive phenotype points to new therapeutic targets. Neoplasia 2005;7:7–16.
21. Phillips HS, Kharbanda S, Chen R, et al. Molecular subclasses of high-grade glioma predict prognosis, delineate a pattern of disease progression, and resemble stages in neurogenesis. Cancer Cell 2006;9:157–73.
22. Sugawa N, Yamamoto K, Ueda S, et al. Function of aberrant EGFR in malignant gliomas. Brain Tumor Pathol 1998;15:53–7.
23. Arwert E, Hingtgen S, Figueiredo JL, et al. Visualizing the dynamics of EGFR activity and antiglioma therapies *in vivo*. Cancer Res 2007;67:7335–42.
24. Lu KV, Zhu S, Cvrljevic A, et al. Fyn and SRC are effectors of oncogenic epidermal growth factor receptor signaling in glioblastoma patients. Cancer Res 2009;69:6889–98.
25. Ying H, Zheng H, Scott K, et al. Mig-6 controls EGFR trafficking and

Published OnlineFirst September 21, 2010; DOI:10.1158/0008-5472.CAN-10-2353

suppresses gliomagenesis. Proc Natl Acad Sci U S A 2008;107:6912–7.
26. Yang W, Wu G, Barth RF, et al. Molecular targeting and treatment of composite EGFR and EGFRvIII-positive gliomas using boronated monoclonal antibodies. Clin Cancer Res 2008;14:883–91.
27. Galli R, Binda E, Orfanelli U, et al. Isolation and characterization of tumorigenic, stem-like neural precursors from human glioblastoma. Cancer Res 2004;64:7011–21.
28. Lee J, Kotliarova S, Kotliarov Y, et al. Tumor stem cells derived from glioblastomas cultured in bFGF and EGF more closely mirror the phenotype and genotype of primary tumors than do serum-cultured cell lines. Cancer Cell 2006;9:391–403.
29. Sok JC, Coppelli FM, Thomas SM, et al. Mutant epidermal growth factor receptor (EGFRvIII) contributes to head and neck cancer growth and resistance to EGFR targeting. Clin Cancer Res 2006;12:5064–73.
30. Singh SK, Hawkins C, Clarke ID, et al. Identification of human brain tumour initiating cells. Nature 2004;432:396–401.
31. Son MJ, Woolard K, Nam DH, Lee J, Fine HA. SSEA-1 is an enrichment marker for tumor-initiating cells in human glioblastoma. Cell Stem Cell 2009;4:440–52.
32. Read TA, Fogarty MP, Markant SL, et al. Identification of CD15 as a marker for tumor-propagating cells in a mouse model of medulloblastoma. Cancer Cell 2009;15:135–47.
33. Reynolds BA, Rietze RL. Neural stem cells and neurospheres—re-evaluating the relationship. Nat Methods 2005;2:333–6.
34. Lee Y, Scheck AC, Cloughesy TF, et al. Gene expression analysis of glioblastomas identifies the major molecular basis for the prognostic benefit of younger age. BMC Med Genomics 2008;1:52.
35. Roesch A, Fukunaga-Kalabis M, Schmidt EC, et al. A temporarily distinct subpopulation of slow-cycling melanoma cells is required for continuous tumor growth. Cell 2006;141:583–94.
36. Sakariassen PO, Prestegarden L, Wang J, et al. Angiogenesis-independent tumor growth mediated by stem-like cancer cells. Proc Natl Acad Sci U S A 2006;103:16466–71.
37. Hynes NE, Lane HA. ERBB receptors and cancer: the complexity of targeted inhibitors. Nat Rev Cancer 2005;5:341–54.
38. Maru SV, Holloway KA, Flynn G, et al. Chemokine production and chemokine receptor expression by human glioma cells: role of CXCL10 in tumour cell proliferation. J Neuroimmunol 2008;199:35–45.
39. Choi K, Benveniste EN, Choi C. Induction of intercellular adhesion molecule-1 by Fas ligation: proinflammatory roles of Fas in human astroglioma cells. Neurosci Lett 2003;352:21–4.
40. Mellinghoff IK, Wang MY, Vivanco I, et al. Molecular determinants of the response of glioblastomas to EGFR kinase inhibitors. N Engl J Med 2005;353:2012–24.
41. Shmelkov SV, Butler JM, Hooper AT, et al. CD133 expression is not restricted to stem cells, and both CD133 and CD133 metastatic colon cancer cells initiate tumors. J Clin Invest 2008;118:2111–20.
42. Ogden AT, Waziri AE, Lochhead RA, et al. Identification of $A2B5^+$ $CD133^-$ tumor-initiating cells in adult human gliomas. Neurosurgery 2008;62:505–14, discussion 514–505.
43. Reya T, Morrison SJ, Clarke MF, Weissman IL. Stem cells, cancer, and cancer stem cells. Nature 2001;414:105–11.
44. Visvader JE, Lindeman GJ. Cancer stem cells in solid tumours: accumulating evidence and unresolved questions. Nat Rev Cancer 2008;8:755–68.
45. Hill RP, Perris R. "Destemming" cancer stem cells. J Natl Cancer Inst 2007;99:1435–40.
46. Brennan C, Momota H, Hambardzumyan D, et al. Glioblastoma subclasses can be defined by activity among signal transduction pathways and associated genomic alterations. PLoS One 2009;4:e7752.
47. Martinez R, Rohde V, Schackert G. Different molecular patterns in glioblastoma multiforme subtypes upon recurrence. J Neurooncol 2005;96:321–9.
48. Haas-Kogan DA, Prados MD, Tihan T, et al. Epidermal growth factor receptor, protein kinase B/Akt, and glioma response to erlotinib. J Natl Cancer Inst 2005;97:880–7.
49. Stommel JM, Kimmelman AC, Ying H, et al. Coactivation of receptor tyrosine kinases affects the response of tumor cells to targeted therapies. Science 2007;318:287–90.